

Thermoelectric effects in STM tunneling through a monoatomic chain

M. Krawiec* and M. Jałochowski

Institute of Physics and Nanotechnology Center, M. Curie-Skłodowska University, pl. M. Curie-Skłodowskiej 1, 20-031 Lublin, Poland

Received 9 September 2006

Key words STM; atomic wire; tunneling

PACS 68.37.Ef, 81.07.Vb, 73.40.Gk

We study thermoelectric properties of the system composed of a monoatomic chain on a surface and additional electrode coupled to the chain, which can be an STM tip. In particular, we are interested in thermopower, electric and thermal conductance, Wiedemann-Franz relation and thermoelectric figure of merit, which is a direct measure of the usefulness of the system for applications. We discuss the modifications of the STM wire topography due to temperature gradient between the electrodes. Finally, we also make connection to STM experiment, in which the thermopower has been directly measured, showing different structure, not visible in topography spectra.

Copyright line will be provided by the publisher

1 Introduction

Since the invention of scanning tunneling microscopy (STM) [1] it became possible to tailor and analyze small nanostructures on various conducting surfaces [2, 3]. As the STM is a real space technique and is very sensitive to local atomic and electronic structures, it has been widely applied to study various surface reconstructions [3] and low dimensional structures, like single atoms [2, 3], islands [4, 5] or one-dimensional monoatomic chains [6]-[9]. While the STM is used to characterize various structures measuring topography or current-voltage characteristics, it is also suitable to get information on thermal properties of the system. For example, local thermopower $S(\mathbf{r})$ of various surfaces has been measured with STM [10, 11]. Thus the topography of the surface can be supplemented by its 'thermal' image. It turns out that the thermal images show features that are not accessible in the conventional STM topographic images. In particular, the maxima of the thermopower in the thermal image of the surface do not overlap with the tunneling current maxima [10, 11]. The local thermopower of the surfaces observed in STM experiments [10, 11] has been also studied theoretically [12] within the Tersoff-Hamann approach [13]. It was found that the magnitude of the thermopower depends on the logarithmic derivative of the local surface density of states at the Fermi level and does not show exponential dependence on tip-surface distance, in contrast to the tunneling current.

The above examples show that thermoelectric properties are the source of information complementary to that obtained from other transport characteristics. In bulk systems, transport in the presence of electrical and thermal gradients is a well studied phenomenon. Recently, it became possible to study those effects, both experimentally and theoretically, in atomic-scale systems, like quantum point contacts [14, 15], quantum dots [16]-[21], quantum dot superlattices [22], quantum wires with end atoms coupled to external leads [23], carbon nanotubes [24, 25] or correlated multilayered nanostructures [26].

* Corresponding author: e-mail: krawiec@kft.umcs.lublin.pl, Phone: +48 81 5376146, Fax: +48 81 5376190

It is the purpose of the present work to study thermoelectric properties of quantum wire in STM geometry. We shall concentrate on the electric and thermal conductance, thermopower and related quantities, like thermoelectric figure of merit which is a direct measure of the usefulness of the system for applications and Wiedemann-Franz ratio which signals breakdown of the Fermi liquid state. We also discuss the modifications of the STM wire topography due to temperature gradient between the electrodes. To explore electric and thermal properties of the system we propose a model of tunneling between STM tip and surface and use equations of motion technique for Green functions. Rest of the paper is organized as follows: in Sec. 2 we introduce our model based on tight binding model and discuss some aspects of our procedure, and the results of our calculations are presented in Sec. 3. We end up with summary and conclusions.

2 The model

Our model system is described by the Hamiltonian

$$H = \sum_{\lambda \in \{t,s\} \mathbf{k} \sigma} \epsilon_{\lambda \mathbf{k}} c_{\lambda \mathbf{k} \sigma}^{\dagger} c_{\lambda \mathbf{k} \sigma} + \sum_{\sigma} \epsilon_0 c_{0 \sigma}^{\dagger} c_{0 \sigma} + \sum_{i \sigma} \epsilon_w c_{i \sigma}^{\dagger} c_{i \sigma} + \sum_{ij \sigma} (t_w c_{i \sigma}^{\dagger} c_{j \sigma} + H.c.) + \sum_{\mathbf{k} \sigma} (V_t c_{t \mathbf{k} \sigma}^{\dagger} c_{0 \sigma} + H.c.) + \sum_{i \mathbf{k} \sigma} (V_{is} e^{i \mathbf{k} \mathbf{R}_i} c_{s \mathbf{k} \sigma}^{\dagger} c_{i \sigma} + H.c.) + \sum_{i \sigma} (t_{i0} c_{0 \sigma}^{\dagger} c_{i \sigma} + H.c.), \quad (1)$$

and consists of N-atom metallic wire with atomic energies ϵ_w and hopping parameter t_w between neighboring wire atoms. The wire is connected to the surface via parameters V_{is} , which we treat as a reservoir for electrons with energies $\epsilon_{s \mathbf{k}}$. STM tip is modeled by single atom with energy ϵ_0 attached to another reservoir (with electron energies $\epsilon_{t \mathbf{k}}$) via coupling V_t . Tunneling between STM tip and the wire atoms is described by tunneling matrix element t_{i0} . As usually, c_{λ}^{\dagger} (c_{λ}) stands for creation (annihilation) electron operator in STM lead ($\lambda = t$), tip atom ($\lambda = 0$), i th wire atom ($\lambda = i$) and surface ($\lambda = s$). Schematic view of our model system is shown in Fig. 1.

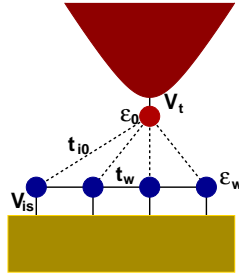


Fig. 1 Schematic view of our model system composed of N-atom wire on surface and STM tip.

In order to calculate tunneling current J_e and thermal flux J_Q flowing from the STM electrode to the rest of the system we follow standard derivation [21] and get

$$J_e = \frac{e}{h} \int d\omega \mathcal{T}(\omega) [f(\omega - \mu_t) - f(\omega - \mu_s)], \quad (2)$$

$$J_Q = \frac{1}{h} \int d\omega \mathcal{T}(\omega) (\omega - \mu_t) [f(\omega - \mu_t) - f(\omega - \mu_s)], \quad (3)$$

where $\mathcal{T}(\omega) = 2\Gamma^t(\omega) \sum_{ij} \Gamma_{ij}^s(\omega) G_{j0}^a(\omega) G_{0j}^r(\omega)$ is the transmittance of the system, $f(\omega)$ is the Fermi distribution function, and μ_t (μ_s) is the chemical potential of the tip (surface) electrode. $G_{j0}^{r(a)}(\omega)$ is the matrix element (connecting the tip atom with the j th wire atom) of the retarded (advanced) Green function $\hat{G}(\omega)$,

the solution of the equation $(\omega\hat{1} - \hat{H})\hat{G}(\omega) = \hat{1}$. The parameter $\Gamma^t(\omega) = \sum_{\mathbf{k}} |V_t|^2 \delta(\omega - \epsilon_{t\mathbf{k}})$ denotes strength of the coupling between the tip atom and STM electrode, while $\Gamma_{ij}^s(\omega) = \sum_{\mathbf{k}} |V_s|^2 e^{i\mathbf{k}(\mathbf{R}_i - \mathbf{R}_j)} \delta(\omega - \epsilon_{t\mathbf{k}}) = \Gamma^s(\omega) \sin(k_F a(i - j)) / (k_F a(i - j))$ is the coupling between wire atoms i and j via the surface. k_F is the Fermi wave vector of the surface electrode, and a is a distance between neighboring wire atoms. In typical metals $k_F a$ is of order of 4 – 5.

For small bias voltages $eV = \mu_t - \mu_s \rightarrow 0$ and small temperature gradients $\delta T = T_t - T_s \rightarrow 0$ one defines conductance $G = -(e^2/T)L_{11}$, thermopower is given in the form $S = -(1/eT)(L_{12}/L_{11})$, and thermal conductance $\kappa = (1/T^2)(L_{22} - L_{12}^2/L_{11})$. The linear response coefficients read

$$L_{11} = \frac{T}{h} \int d\omega \mathcal{T}(\omega) \left(\frac{\partial f(\omega)}{\partial \mu} \right)_T, \quad (4)$$

$$L_{12} = \frac{T^2}{h} \int d\omega \mathcal{T}(\omega) \left(\frac{\partial f(\omega)}{\partial T} \right)_\mu, \quad (5)$$

$$L_{22} = \frac{T^2}{h} \int d\omega \mathcal{T}(\omega) (\omega - \mu_t) \left(\frac{\partial f(\omega)}{\partial T} \right)_\mu. \quad (6)$$

3 Results and discussion

Before the presentation of numerical results, we would like to comment on choice of the model parameters used in the present work. In numerical calculations we have assumed equal and energy independent coupling parameters ($\Gamma^{t(s)}(\omega) = \Gamma^{t(s)}$) and chosen $\Gamma^s = \Gamma^t = \Gamma$ as an energy unit. The other parameters have been chosen in order to satisfy realistic situation in experiments. The hopping integral along the wire is $t_w = 2$, the parameter connecting tip with underneath wire atom $t_{i0} = 0.1$ and STM tip and wire atomic energies $\varepsilon_0 = \varepsilon_w = 0$. For example, taking $\Gamma = 0.05$ eV, we get $t_w = 0.1$ eV and $t_{i0} = 0.005$ eV. Such a value of t_{i0} gives tip-surface distance $z_{i0} = 6$ Å. Also temperature is measured in units of Γ ($k_B = 1$) and for example, $T = 1$ corresponds to ≈ 500 K.

Figure 2 shows conductance G (top panels), thermal conductance κ (middle panels) and thermopower S (bottom panels) of quantum wire. The temperature dependencies of those quantities for wires consisted of different number of atoms (indicated in the figure) are shown in left panels, while in right panels the same quantities are plotted as a function of number of atoms in the wire at different temperatures. In all the cases the STM tip is above first wire atom, and the tip-surface distance is equal to 6 Å.

The conductance G shows rather an expected behavior, i.e. at high T it goes like T^{-1} , while in the low temperature regime remains constant. Note, that it never reaches unitary limit ($2e^2/h$) due to large tip surface distance. However there are differences in maximal values of G for different number of atoms N in the wire. To be more precise, the conductance shows even-odd oscillations with increasing N (see right top panel). Such a behavior is similar to that observed in the transport along wires [27]. Similar oscillations shows thermal conductance κ , although they are less pronounced at higher temperatures (see right middle panel). However, it has different temperature dependence, it goes linearly with T at low temperatures, while at high T shows T^{-2} behavior. The thermopower S goes linearly to zero with T and behaves like T^{-1} in high temperature regime. It is almost always positive in the whole range temperatures, suggesting an electron nature of transport. Interestingly, it shows also even-odd oscillations with number of atoms in a wire but with opposite phase to G and κ , i.e. while G and κ show maxima for the wires composed of odd number of atoms, S has maximal values for even N . This can be easily understood, as the conductance G is sensitive to density of states (DOS) at the Fermi level E_F , while S reflects the curvature of DOS around it. In odd atom wire the DOS is large at E_F and has small curvature, while in even atom wire the situation is opposite. Note that the presence of the surface introduces asymmetry to the DOS around the Fermi energy, even if we assume wire energies to coincide with E_F [28, 9].

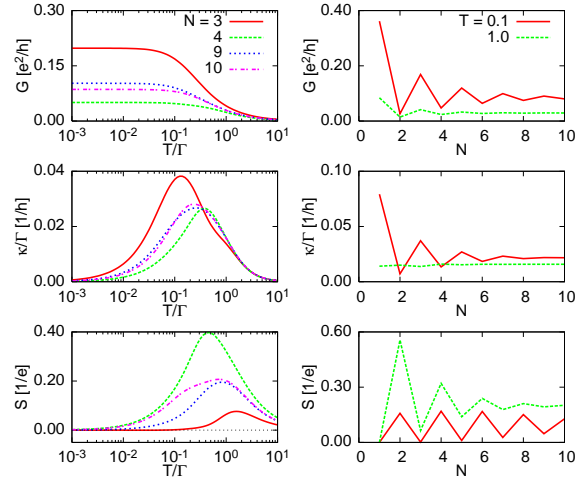


Fig. 2 Conductance (top panels), thermal conductance (middle panels) and thermopower (bottom panels) as a function of temperature (left panels) and as a function of number of atoms in the wire (right panels). All the curves correspond to situation when STM tip is placed above first wire atom, and the tip surface distance is equal to 6 \AA .

Topography of the wire consisted of $N = 19$ atoms at $eV = 0.1$ and $J_e = 10^{-5}$ ($V = 0.5$ mV and $J_e = 0.2$ nA) is shown in Fig. 3. Dashed line corresponds to the situation when STM tip and the surface

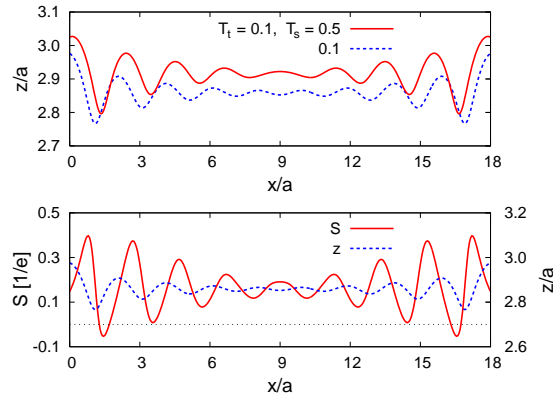


Fig. 3 Topography of the wire $z(x)$ at $eV = 0.1$ and $J_e = 10^{-5}$ ($V = 0.5$ mV and $J_e = 0.2$ nA) for the STM tip temperature $T_t = 0.1$ and different temperatures of the surface electrode T_s (top panel). Corresponding thermopower $S(x)$ is shown in the bottom panel. For comparison $z(x)$ is also displayed. x and z are in units of the distance between neighboring wire atoms a .

temperatures are equal ($T_t = T_s = 0.1$ (50 K)), while the solid one to the situation when surface is at elevated temperature $T_s = 0.5$ (250 K). The reverse of the topography is clearly seen due to the temperature difference between STM tip and the surface. To be convinced that this is really the case, we have also shown thermopower $S(x)$ (solid line in the bottom panel). Note that the maxima of $S(x)$ do not coincide with the topography maxima calculated for $T_t = T_s$ (dashed line in the bottom panel) but they do with those obtained at different STM tip and surface temperatures (dashed line in the top panel). Thus indeed the reverse of the topography is caused by the temperature gradient between STM tip and surface. Similar differences between the topography and thermal images of the surface have been observed experimentally with STM [11].

The Wiedemann-Franz (WF) relation $\kappa/TG = \pi^2/3e^2$ describes transport in Fermi liquid bulk metals and in general is not obeyed in mesoscopic systems. In our system there are no Coulomb interactions and this relation is fulfilled at low temperatures, thus indicating Fermi liquid ground state. This can be also understood from temperature behavior of electric and thermal conductances, as κ decreases linearly with T, while G remains constant. At high temperatures the WF relation is violated due to large fluctuations of G, which are of order of $2e^2/h$ [29].

Finally, we would like to comment on usefulness of such systems for potential applications, like thermoelectric power generators or cooling systems [22]. A direct measure of it is thermoelectric figure of merit $Z = S^2G/\kappa$. For simple systems it is inversely proportional to operation temperature, thus conveniently consider ZT, which numerical value is a measure of the system performance. In our system the value of ZT is always smaller than 1, indicating limited practical applicability. Also the thermopower, which is of order of 10^{-2} mV/K, leads to similar conclusions.

4 Conclusions

In conclusion we have studied thermal properties of monoatomic quantum wire in STM geometry, and show differences between topography and thermal images of the wire. In particular, the maxima of calculated thermopower along the wire do not coincide with those of topography spectra due to the fact that tunneling current is sensitive to the density of states, while thermopower is sensitive to the slope of the density of states at the Fermi energy. We discussed also Wiedemann-Franz relation and found that is fulfilled at low temperatures indicating Fermi liquid ground state.

Acknowledgements This work has been supported by the Grant No 1 P03B 004 28 of the Polish Committee of Scientific Research.

References

- [1] G. Binnig *et al.*, Appl. Phys. Lett. **40** (1982) 178; Phys. Rev. Lett. **49** (1982) 57.
- [2] G. A. D. Briggs, A. J. Fisher, Surf. Sci. Rep. **33** (1999) 1.
- [3] W. A. Hofer *et al.*, Rev. Mod. Phys. **75** (2003) 1287.
- [4] M. Jałochowski, Prog. Surf. Sci. **74** (2003) 97.
- [5] M. Krawiec *et al.*, Surf. Sci. **600** (2006) 1641.
- [6] F. J. Himpsel *et al.*, J. Phys.: Condens. Matter **13** (2001) 11097.
- [7] J. N. Crain *et al.*, Phys. Rev. **B69** (2004) 125401.
- [8] M. Jałochowski *et al.*, Appl. Surf. Sci. **211** (2003) 209.
- [9] M. Krawiec *et al.*, phys. stat. sol. (b)**242** (2005) 332; Phys. Rev. **B73** (2006) 075415.
- [10] J. M. Weaver *et al.*, Nature **342** (1989) 783.
- [11] C. C. Williams, H. K. Wickramasinghe, Nature **344** (1990) 317.
- [12] J. A. Stovneng, P. Lipavsky, Phys. Rev. **B42** (1990) 9214.
- [13] J. Tersoff, D. R. Hamann, Phys. Rev. Lett. **50** (1983) 1998; Phys. Rev. **B31** (1985) 805.
- [14] H. van Houten *et al.*, Semicond. Sci. Technol. **7** (1992) B215.
- [15] L. W. Molenkamp *et al.*, Phys. Rev. Lett. **68** (1992) 3765.
- [16] C. W. J. Beenakker, A. A. M. Staring, Phys. Rev. **B46** (1992) 9667.
- [17] A. A. M. Staring *et al.*, Europhys. Lett. **22** (1993) 57.
- [18] D. Boese, R. Fazio, Europhys. Lett. **56** (2001) 576.
- [19] B. Dong *et al.*, J. Phys. Condens. Matter **14** (2002) 11747.
- [20] R. Scheibner *et al.*, Phys. Rev. Lett. **95** (2005) 176602; cond-mat/0608193.
- [21] M. Krawiec, K. I. Wysokiński, Phys. Rev. **B73** (2006) 075307; Physica **B378-380** (2006) 933.
- [22] J. P. Heremans *et al.*, Phys. Rev. **B70** (2004) 115334.
- [23] R. Fazio *et al.*, Phys. Rev. Lett. **80** (1998) 5611.
- [24] M. F. Lin *et al.*, Phys. Rev. **B53** (1996) 11186.
- [25] E. Pop *et al.*, cond-mat/0609075.
- [26] J. K. Freericks *et al.*, cond-mat/0609112.
- [27] N. Agrait *et al.*, Phys. Rep. **377** (2003) 81.
- [28] D. M. Newns, N. Read, Adv. Phys. **36** (1987) 799.
- [29] M. G. Vavilov, A. D. Stone, Phys. Rev. **B72** (2005) 205107.